Molecular Biology of the Cell
Vol. 12, 795–808, April 2001

Golgi Complex Reorganization during Muscle Differentiation: Visualization in Living Cells and Mechanism

Zhuomei Lu,* Donald Joseph,* Elisabeth Bugnard,* Kristien J. M. Zaal,† and Evelyn Ralston*‡

*Laboratory of Neurobiology, National Institute of Neurological Disorders and Stroke, and †Cell Biology and Metabolism Branch, National Institute of Child Health and Human Development; National Institutes of Health, Bethesda, Maryland 20892-4062

Submitted October 17, 2000; Revised December 27, 2000; Accepted February 2, 2001
Monitoring Editor: Jennifer Lippincott-Schwartz

During skeletal muscle differentiation, the Golgi complex (GC) undergoes a dramatic reorganization. We have now visualized the differentiation and fusion of living myoblasts of the mouse muscle cell line C2, permanently expressing a mannosidase-green fluorescent protein (GFP) construct. These experiments reveal that the reorganization of the GC is progressive (1–2 h) and is completed before the cells start fusing. Fluorescence recovery after photobleaching (FRAP), immunofluorescence, and immunogold electron microscopy demonstrate that the GC is fragmented into elements localized near the endoplasmic reticulum (ER) exit sites. FRAP analysis and the ER relocation of endogenous GC proteins by phospholipase A2 inhibitors demonstrate that Golgi-ER cycling of resident GC proteins takes place in both myoblasts and myotubes. All results support a model in which the GC reorganization in muscle reflects changes in the Golgi-ER cycling. The mechanism is similar to that leading to the dispersal of the GC caused, in all mammalian cells, by microtubule-disrupting drugs. We propose that the trigger for the dispersal results, in muscle, from combined changes in microtubule nucleation and ER exit site localization, which place the ER exit sites near microtubule minus ends. Thus, changes in GC organization that initially appear specific to muscle cells, in fact use pathways common to all mammalian cells.

INTRODUCTION

Differentiation and fusion of muscle cells into multinucleated myotubes is accompanied by a dramatic reorganization of the Golgi complex (GC; Tassin *et al.*, 1985b; Ralston, 1993). The classic, compact juxtanuclear GC of the undifferentiated myoblasts appears to disperse into elements that form a fenestrated belt around each of the myotube nuclei and extend between the nuclei. It is known that the reorganization of the GC accompanies a redistribution of the microtubule-nucleating center (Tassin *et al.*, 1985a), and that microtubule-disrupting drugs such as nocodazole disperse the GC of myoblasts but do not affect the GC of myotubes (Tassin *et al.*, 1985b). Even in the absence of fusion, the changes in GC organization do take place in muscle cells that differentiate (Ralston, 1993).

It has long been known that localization of the GC depends on microtubules and that microtubule disruption causes its dispersal (Robbins and Gonatas, 1964; Rogalski and Singer, 1984). Energy requirements rule out that this dispersal simply involves diffusion of fragments (Turner and Tartakoff, 1989). In the past few years, the fragmentation of the GC caused by microtubule disruption has been explained as reflecting a constant recycling of Golgi proteins, retrogradely to the endoplasmic reticulum (ER) and then anterogradely back to the GC. Retrograde trafficking was first described in brefeldin A (BfA)-treated cells (Doms *et al.*, 1989; Lippincott-Schwartz *et al.*, 1989) and subsequently shown to take place constitutively in the absence of drugs (Cole *et al.*, 1998; Drecktrah and Brown, 1999; Zaal *et al.*, 1999). Using nocodazole, Cole *et al.* (1996a) showed that microtubules are not necessary for GC proteins to move retrogradely to the ER. However, when GC proteins emerge from the ER, at the ER exit sites (also called ER export sites; Bannykh *et al.*, 1996), they cannot return toward the centrosome, because microtubules are necessary for this step. In

‡ Corresponding author. E-mail address: ralstone@ninds.nih.gov.
Abbreviations used: BfA, brefeldin A; ER, endoplasmic reticulum; FRAP: fluorescence recovery after photobleaching; GFP, green fluorescent protein; GC, Golgi complex; man, α-mannosidase II; ONO, 2-(p-amylcinnamoyl)amino-4-chlorobenzoic acid (ONO-RS-082); PLA2, phospholipase A2.

the absence of microtubules the GC proteins then reform small stationary stacks of cisternae. The result is an apparent fragmentation of the GC into small stacks found at the ER exit sites. This model is supported by work on live cells expressing GC-localized green fluorescent protein (GFP) constructs (Storrie *et al.*, 1998) and by the finding that phospholipase A2 (PLA2) inhibitors that block retrograde trafficking (de Figueiredo *et al.*, 1998) prevent the nocodazole-induced GC dispersal (Drecktrah and Brown, 1999). Retrograde trafficking has recently been proposed to explain the disassembly of the GC during mitosis (Zaal *et al.*, 1999), which was, so far, understood to result from fission of the GC (Lucocq and Warren, 1987; Shima *et al.*, 1998).

We now examine the possibility that the changes in GC organization during muscle differentiation also reflect the cycling of Golgi proteins through the ER. Because nothing was known either of the timing of the GC changes in relation to other events of myogenesis, or of their duration, we first sought to observe the process in live cells. We have isolated a subclone of the mouse muscle cell line C2 (Yaffe and Saxel, 1977) that permanently expresses a GFP-tagged construct of α-mannosidase II, a resident GC protein. Confocal time-lapse recordings of the GFP fluorescence of these cells have provided, for the first time, a view of the GC dynamics as the cells move, differentiate, and fuse. To determine whether the elements of the myotube GC are independent from one another as suggested by their immunofluorescent pattern, we have then analyzed the recovery of α-mannosidase II (man)-GFP after photobleaching (FRAP) in myoblasts and myotubes. We have localized the GC fragments in relation to the ER exit sites, and both GC elements and ER exit sites in relation to microtubule nucleation sites. Using FRAP on the transfected cells and treatment with PLA2 inhibitors on untransfected cells, we have shown that the Golgi-ER cycling takes place in both myoblasts and myotubes. Our results are compatible with a model in which changes in microtubule nucleation during differentiation prevent the reformation of a central GC during Golgi-ER cycling.

MATERIALS AND METHODS

Antibodies and Reagents

Mouse anti-giantin, rabbit anti-GM130, anti-mannosidase, anti-Sec13p, anti-p137/Sec31p, and anti-tyrosylated-α-tubulin were the generous gifts of Drs. Adam Linstedt (Mellon Institute, Pittsburgh, PA), Graham Warren (Yale University, New Haven, CT), Kelley Moremen (University of Georgia, Athens, GA), Wanjin Hong (National University of Singapore, Singapore), Fred Gorelick (Yale University), and George Cooper IV (Veterans Administration Medical Center, Charleston, SC), respectively. Mouse anti-GM130 was purchased from Transduction Labs/BD PharMingen (San Diego, CA), mouse anti-α-tubulin DM1A from Sigma (St. Louis, MO), and rabbit anti-GFP from Clontech Laboratories (Palo Alto, CA). Fluorescently labeled secondary antibodies were purchased from Organon-Teknika (Durham, NC) and Jackson ImmunoResearch (West Grove, PA). Nanogold-conjugated secondary antibodies as well as silver enhancement kits were purchased from Nanoprobes (Stony Brook, NY). Hoechst 33342 (bis-benzimide), cycloheximide, and nocodazole were purchased from Sigma. Stock solutions of 20 mg/ml cycloheximide and 5 mg/ml nocodazole in DMSO were stored at −20°C. Brefeldin A was purchased from Epicentre Biotechnologies (Madison, WI). A 1-mg/ml stock solution in ethanol was kept at 4°C. PLA2 antagonist 2-(p-amylcinnamoyl)amino-4-chlorobenzoic acid (ONO-RS-082; referred to as ONO) was purchased from Biomol Research Laboratories (Plymouth Meeting, PA). Stock solutions of 50 mM in DMSO were stored at −20°C and diluted to a final concentration of 15 and 25 μM.

Plasmids

Mannosidase-$(GFP)_3$, a construct encoding α-mannosidase II with three eGFPs in tandem, has been described by Zaal *et al.* (1999)

C2 Culture and Transfection

The C2 cells used here are a subclone of C2C12. They are plated on tissue culture dishes or on glass coverslips coated with 0.2% gelatin in medium containing 20% fetal bovine serum, 0.5% chick embryo extract, 2 mM Glutamax in Dulbecco's modified Eagle medium (DMEM), 1 g/l glucose (growth medium). When the cells reach ~70% confluence, normally within 48 h, the growth medium is replaced by fusion medium (4% horse serum, 2 mM Glutamax in DMEM). Half of the medium is replaced daily. Glass coverslips are routinely covered with a carbon coat before the gelatin, to improve adhesion of the spontaneously contracting myotubes. For recordings from live cultures, C2 were plated either on glass coverslips sealed with Sylgaard (Dow Corning, Midland, MI) to the bottom of a 35-mm tissue culture dish pierced with a 12-mm-diameter hole, or on 4-cm-diameter glass coverslips.

For permanent transfections, 4×10^5 cells were plated in 15-cm dishes and transfected 24 h later with *N*-[1-(2,3-dioleoyloxy)propyl]-*N,N,N*-trimethylammonium methylsulfate (DOTAP) (Roche Molecular Biochemicals, Indianapolis, IN). DOTAP (90 μl) was diluted to 300 μl with 20 mM HEPES, 150 mM NaCl (HN; pH 7.27 adjusted with NaOH; osmolarity = 320–330). DNA (10 μg) was diluted to 150 μl with HN. DNA and DOTAP were mixed and left for 10 min at room temperature. The cells were washed with HN, and covered with the DNA-DOTAP suspension. After 5 h in the CO_2 incubator they were transferred to growth medium. After 48 h, medium was supplemented with 400 μg/ml active Geneticin (G418; Life Technologies, Grand Island, NY). After 10 d, G418-resistant cells were pooled and examined. About 20% of the cells expressed useable levels of the GFP construct. In a further step, they were replated at clonal density and ~100 clones were picked. Several clones showing relatively uniform expression of the GFP construct were grown in 100 μg/ml G418 and further tested. We verified that the transfected cells resembled the parent cell line in growth and morphological characteristics, and fused normally. After fusion, myotubes were labeled for 90 min at 37°C with Texas Red-conjugated α-bungarotoxin (Molecular Probes, Eugene, OR) to verify the presence on the cell surface of clusters of acetylcholine receptors, as an indicator of proper functioning of the Golgi complex (Gu *et al.*, 1989). One clone was retained for further studies. For treatments with the PLA2 inhibitor ONO, the cells were rinsed and placed in serum-free medium because serum blocks the effects.

Immunofluorescent Staining

Standard immunofluorescence procedures were followed as detailed in Ralston and Ploug (1996). Cells were permeabilized with 0.04% saponin (Sigma) present throughout except for microtubule staining experiments in which no further detergent was necessary after the Triton X-100 extraction. To observe microtubule nucleation sites, myotubes (2 d in fusion medium) were kept on ice for 15 min, and then warmed up at 37°C in fresh fusion medium containing 5 μg/ml nocodazole. After 1 h, cultures were briefly washed with fusion medium, left at 37°C for 5 min recovery, and fixed in a microtubule-stabilizing buffer (4% paraformaldehyde, 3% sucrose, 60 mM piperazine-*N,N*′-bis(2-ethanesulfonic acid), 25 mM HEPES, 10 mM EGTA, 2 mM $MgCl_2$, 1% Triton X-100 in water at pH = 6.9) for 30 min.

Light Microscopy

Conventional microscopy was done with a Leica DMRD microscope (Leica, Deerfield, IL). Digital images were collected with a Sensys charge-coupled device camera (Photometrics, Tucson, AZ). Images were adjusted for contrast with Photoshop 5.5 and printed from a MacIntosh G3 computer on a Pictrography 3000 digital printer (Fuji, Elmsford, NY). Confocal images were obtained on Zeiss LSM 410 and 510 at the National Institute of Neurological Disorders and Stroke Light Imaging Facility, and then transferred to a MacIntosh computer for observation and analysis.

For overnight time-lapse recordings, the coverslip was placed in a Focht Live-Cell Chamber System (FCS2; Bioptechs, Butler, PA) on the stage of the LSM 410 confocal microscope and imaged in phenol red-free medium supplemented with 20 mM HEPES pH 7.4 at 37°C. To maximize the chances of observing differentiation and fusion in the unsynchronized live cultures, imaging was started after 6–12 h in fusion medium, at a large time interval (15 min) and a magnification that allowed us to observe a large field (zoom 1.0 with a 63× N.A. 1.4 oil immersion lens, which gives a field of ~200 × 200 μm). Up to six positions were marked and stored. Every 15 min a cycle of recordings was started. After automatic focusing on the glass-cell interface, two optical sections 1 μm apart were recorded for each position at each time point. Stacks of images, including a maximum projection of the two planes or a single plane, were created in NIH Image for quantitation and conversion into Quicktime movies. NIH Image is written by Wayne Rasband at the National Institutes of Health and freely available from the Internet at http://rsb.info.nih.gov/nih-image/.

FRAP was done at 37°C in the Zeiss LSM 510 confocal microscope as described by Cole *et al.* (1996b) and Ellenberg *et al.* (1997). Recordings were carried out with a 63× N.A. 1.4 oil immersion lens. Photobleaching was obtained by scanning the region of interest, which was either a 2- to 4-μm-wide rectangular box or a hand-drawn box the contours of which surrounded the element to bleach, at full power and 100% transmission. Recovery was followed by scanning the whole cell at lower power (~40%) and attenuated transmission (10 or 3%) at intervals from 10 s to 5 min. We verified that the bleaching extended throughout the cell by observing Z-sections immediately after bleaching control cells. The actual width of the bleached area was measured by photobleaching of fixed cells. The data were quantitated by measuring the mean fluorescence intensity of the bleached area with NIH Image. Data were transferred to Excel and for each data point the fluorescence intensity I_t was expressed as percentage of the initial mean fluorescence intensity before bleaching, I_{t0}. The diffusion coefficient D was estimated by fitting the data to the equation $I_t = I_{tf}\{1 - [w^2(w^2 + 4\pi Dt)^{-1}]^{1/2}\}$ where w is the width of the bleached region (in microns) and I_{tf} is the intensity of the signal at the end of the recovery period. Data fitting was done with Kaleidagraph (Synergy Software, Reading, PA) on the Macintosh. The assumptions involved in the use of this equation and its limitations have been discussed by Ellenberg *et al.* (1997). The percentage of mobile fraction was calculated as $\% = (I_{tf} - I_{min})/(I_{t0} - I_{min})$ where I_{min} is the mean fluorescence intensity immediately after the bleach and I_{tf} is the mean fluorescence intensity after maximum recovery. Because the repetitive recordings at 10- to 30-s intervals caused some bleaching of the whole GC (10–30%), the value for I_{tf} was corrected to take into account photobleaching of control areas. For slow recovery experiments, images were collected every minute or every 5 min. All photobleaching experiments were carried out in the presence of 25 μM cycloheximide added 30 min before the start of the recordings to rule out contribution from new protein synthesis. Photobleaching experiments were repeated in six independent sessions.

Electron Microscopy (EM)

For conventional EM, cultures were fixed with 4% glutaraldehyde, treated with 1% osmium, embedded in Epon, and sectioned according to standard procedures. For immunogold labeling, cultures were fixed with 2% formaldehyde (from a 16% stock; EMS, Ft. Washington, PA) in 0.1 M phosphate buffer for 20 min at 37°C, then for 40 min at room temperature, and then stained as for immunofluorescence, except that the secondary antibody was a gold-conjugated Fab. Silver enhancement with the HQ kit was done according to the manufacturer's protocol. Subsequent treatments were as described in Ralston and Ploug (1996).

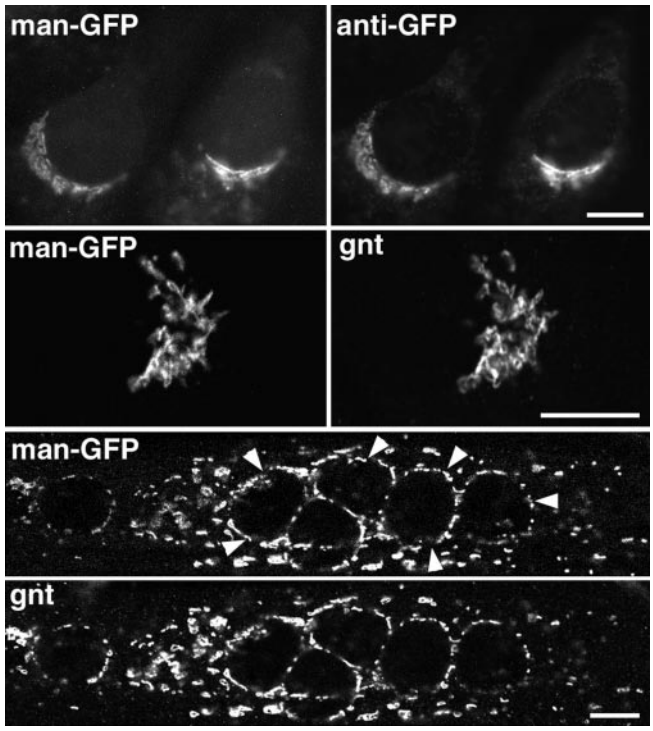

Figure 1. Mannosidase-GFP localizes to the GC of myoblasts and myotubes. Cultures from a C2 subclone that permanently express man-GFP were stained with an anti-GFP antibody and observed in a conventional fluorescence microscope (top row). In most cells, >95% of the anti-GFP staining colocalizes with the GFP fluorescence in the Golgi complex. The cultures were also labeled with anti-giantin (gnt) to label the GC and observed in the confocal microscope. The second row shows the classic, polar GC in a single myoblast (the nucleus, which does not show, is to the left of the GC); the bottom panels show the dispersed GC in a multinucleated myotube. Golgi elements encircle the nuclei (arrowheads) and are found in the cytoplasm. Notice the similarity of the man-GFP and giantin patterns in both myoblasts and myotubes. Bars, 10 μm.

RESULTS

Observation of Differentiation and Fusion in Living Cells

C2 myoblasts permanently expressing a man-GFP construct grow, differentiate, and fuse normally (see MATERIALS AND METHODS). The GFP fluorescence is appropriately localized to the Golgi complex of both undifferentiated and differentiated cells, and in most cells >95% of the GFP detected by an anti-GFP antibody is in the Golgi complex (Figure 1).

To observe the GC in myoblasts before and during fusion, which occurs stochastically in these unsynchronized cul-

tures, sequences of confocal fluorescence images were recorded at 15-min interval, 6 to 12 h after switching the cultures from growth to fusion medium. Analysis of the recordings showed two main phenotypes among the myoblasts. One population of cells was moving at an average speed of 17 μm/h (range 3–46 μm/h, measured on 28 cells in 6 separate recordings). The GC of these cells appeared mostly compact and polar but was constantly changing shape and occasionally surrounded the nucleus as the cells moved (Figure 2A). In animated sequences of images, the movement often resembles the breaststroke of a swimmer with the GC pointing in the direction of the movement ahead of the nucleus (see accompanying videos of Figure 2, A and B). The other population of cells was less motile (average speed 5 μm/h, range 2–11 μm/h, measured on 18 cells from 6 separate recordings). Its GC was perinuclear, circling the whole nucleus, and did not revert to a polar shape. One of these cells appears in the fourth panel (3 h) of Figure 2A. A small minority of cells showed a GC made of fragments that did not form a perinuclear ring (Figure 2D). We observed >20 events of myoblasts fusing to other myoblasts (Figure 2B) or to already formed myotubes (Figure 2C). The fusion was accompanied in every case by the near coalescence of the two nuclei (Figure 2B, 2 h 45 min), which was easy to detect. The nuclei remained in a tight embrace for several hours, during which some realignment of the Golgi elements took place (Figure 2B, 4 h 30 min to 7 h 15 min) and only then did the nuclei separate and the elongated shape of the myotube become noticeable. This observation made it clear that only those slow-moving cells with a perinuclear or fragmented GC are competent to fuse and that the permanent change of a polar to a perinuclear organization is progressive (Figure 2, D and E), generally taking >1 h. A reduction in cell motility was observed whenever the GC of a cell lost its polar organization, whether differentiating or not. The formation of rows of Golgi elements between nuclei took place as the myotubes elongated (Figure 2B, final panel) but some differentiated myoblasts already show a comet tail of Golgi elements next to the nucleus (Figure 2, A and E). The transition of the GC from polar to perinuclear is thus completed before fusion takes place.

Lack of Fast Photobleaching Recovery in Myotubes Shows a Break in GC Continuity during Differentiation

To determine whether GC elements of myotubes are interconnected, we observed the recovery after photobleaching of man-GFP. The cultures were treated with cycloheximide to rule out that new protein synthesis contributes to the recovery. When a 2-μm-wide band of the GC was photobleached in live myoblasts, there was a rapid recovery (Figure 3A). The mobile fraction was 56 ± 13% (mean ± SD; n = 6) with a diffusion coefficient of 0.3–0.6 10^{-10} cm^2 s^{-1} (see MATERIALS AND METHODS). In myotubes, we took advantage of the possibility to photobleach hand-drawn regions (Figure 3B). When only a part of an element was bleached (arrows), recovery, as expected, was rapid. In contrast, fully bleached elements (arrowheads) did not recover, showing that they are not connected. We conclude that, in agreement with the fragmented immunofluorescent pattern, the GC looses its continuity during differentiation.

Evidence for Constitutive Golgi-ER Cycling

If there is constitutive Golgi-ER cycling, a fraction of man-GFP should be in the ER at any time (Zaal *et al.*, 1999). To verify this hypothesis, we photobleached the whole GC of myoblasts. The observation of a slow recovery that reached a plateau of ~15% of the original staining after 20 min (Figure 3C) confirmed the existence of a man-GFP source outside the GC. Cycloheximide was routinely added 30–60 min before the photobleaching was done to rule out the contribution of new protein synthesis. Conversely, repeated photobleaching of the ER led to a loss of GC fluorescence of 70% after 90 min (our unpublished results), indicating that the GC serves as a source of man-GFP for the ER. In myotubes, the geometry of GC and ER made their complete selective bleaching difficult. Instead, we photobleached all the elements from wide myotube segments (Figure 3D). Again, a limited and slow recovery was observed (18% in 35 min in the example shown). We conclude that there is a constant slow exchange of resident GC proteins between the GC and ER of both myoblasts and myotubes. Fusion of an unbleached to a bleached Golgi element could theoretically also explain the recovery in myotubes. However, fusion of elements is rare (our unpublished results).

To obtain additional evidence for Golgi-ER cycling, we observed the pattern of the endogenous GC proteins mannosidase and giantin in untransfected cultures treated with the PLA2 inhibitor ONO. Drecktrah and Brown (1999) have shown that ONO prevents nocodazole-induced fragmentation of the GC by blocking anterograde traffic of proteins out of the ER. When C2 cultures were treated with 15 μM ONO for 2 h, mannosidase and giantin were redistributed to the ER in both myoblasts and myotubes (Figure 4), indicating that endogenous GC proteins constantly cycle through the ER both before and after differentiation.

Golgi Elements of Myotubes Are Localized near ER Exit Sites, Which Are Themselves Reorganized during Differentiation

Next, we wanted to determine whether Golgi elements of myotubes are located at the ER exit sites, as are the Golgi complex fragments in nocodazole-treated cells. The ER exit (or export) sites can be defined operationally as the places where small stacks of Golgi cisternae are found in nocodazole-treated cells (Cole *et al.*, 1996a). They have also been characterized morphologically (Bannykh *et al.*, 1996) as areas where COPII-coated budding zones from several ER cisternae congregate. The COPII complex has also been characterized molecularly (Barlowe, 1998).

C2 cultures were treated with BfA to redistribute Golgi proteins to the ER, and then allowed to recover in either normal medium or in the presence of nocodazole to block the Golgi proteins at the ER exit sites, and stained with anti-giantin. In myoblasts (Figure 5, a and b), the GC proteins redistributed to the ER during the BfA treatment, and to disperse sites corresponding to the ER exit sites after recovery in the presence of nocodazole (Figure 5b). In contrast, recovery in normal medium led to a return to the original compact pattern. In myotubes, however, the distribution of giantin to perinuclear and cytoplasmic fragments was observed in nocodazole-treated and in control cells (Figure 5, c and e) as well as in cells recovered from BfA

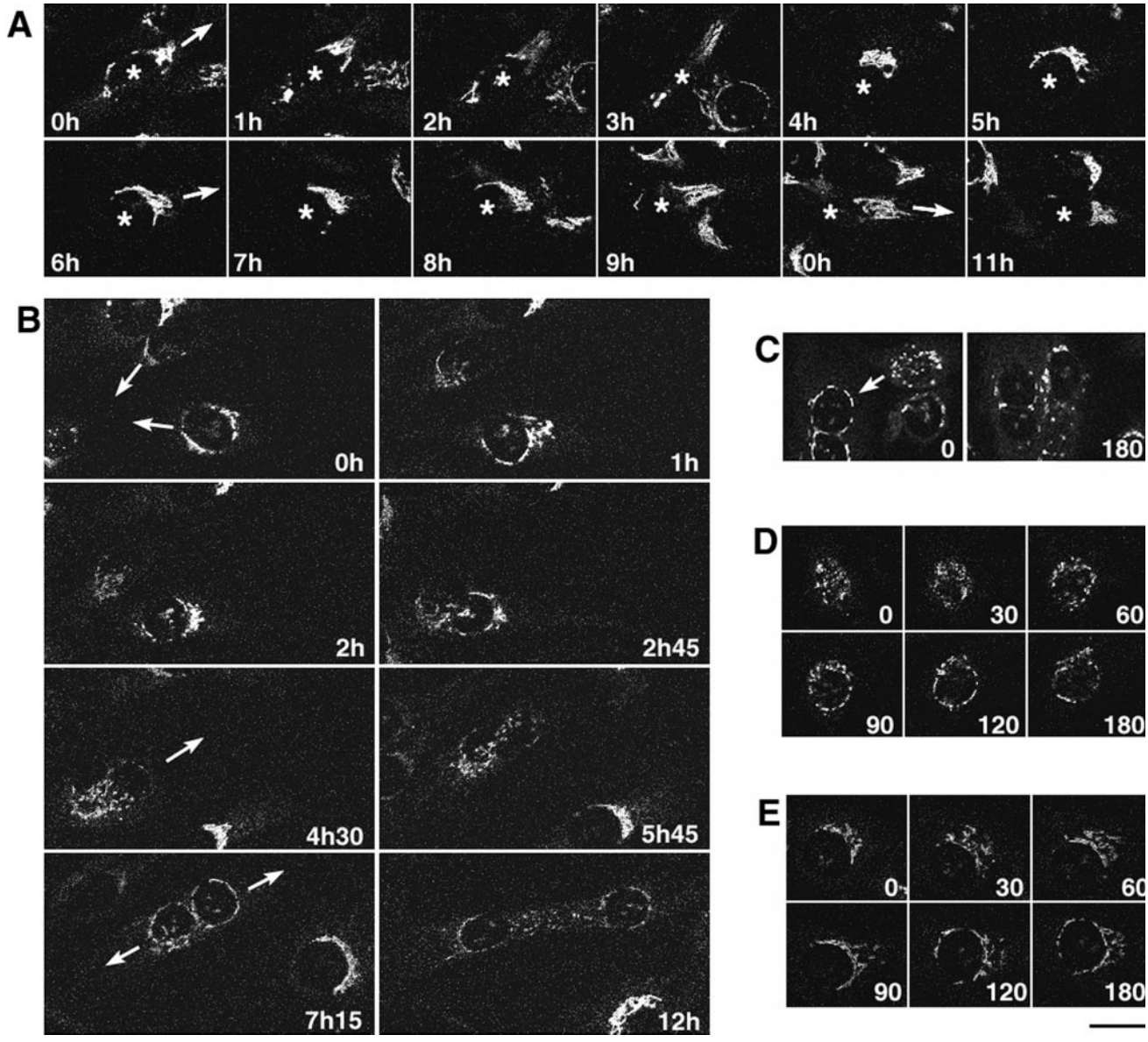

Figure 2. Golgi complex dynamics in C2 myoblasts and during fusion. Cultures of C2-man-GFP recently switched to fusion medium (<12 h) were placed in a sealed chamber on the heated stage of the LSM 410 confocal microscope. Images were recorded every 15 min. The sequences shown illustrate that the GC of motile, undifferentiated myoblasts is constantly reorganizing (A); that the main changes in GC organization are completed before fusion (B and C), and that these changes are progressive (D and E). The time scale is in hours in A–B and in minutes in C–E. See text for more details and video supplement for Quicktime movies of A and B. (A) Each panel comes from a different area of a larger image (the cell that is followed is marked with an asterisk over its nucleus in each panel; it moved ~200 μm during the recordings, eventually going out of view). During the first 3 h, part of the GC is found alongside and behind the nucleus; most of it is ahead of the nucleus and is extending in the direction of the movement (indicated by arrows). Between 3 and 4 h the GC snaps back into a compact shape. In the following hours, it starts extending again, and then contracts back after 10 h. The "3 h" panel shows a second cell, the GC of which is perinuclear. This cell is left behind in the next panel. (B) At the beginning of the recording, two myoblasts are moving toward one another (arrows). The GC of one of them is already perinuclear, whereas the GC of the other still has a polar, compact shape, which progressively changes over the next 2 h. After 2 h 30 min, they fuse. It takes several hours for the nuclei to start separating (7 h 15 min) and the myotube to elongate. The motility of the cells involved was low and the panel shown represents a constant part of the larger field of view. (C) Shown here are two panels from a sequence including the fusion between a myoblast (on the right side at time zero), which slowly moves in the direction of the arrow, to fuse with the myotube (vertical, on the left side). Notice that the GC of the myoblast is completely fragmented in the initial image, before contact and fusion with the myotube. Another myoblast moves out of the field during the recordings. (D and E) Each sequence shows a presumably differentiating myoblast, which is practically immobile and shows slow progressive changes in GC distribution. In the hours following these panels, the GC organization did not change noticeably. The cell in D was approaching another cell with a perinuclear GC when the recording was interrupted. Bar, 10 μm.

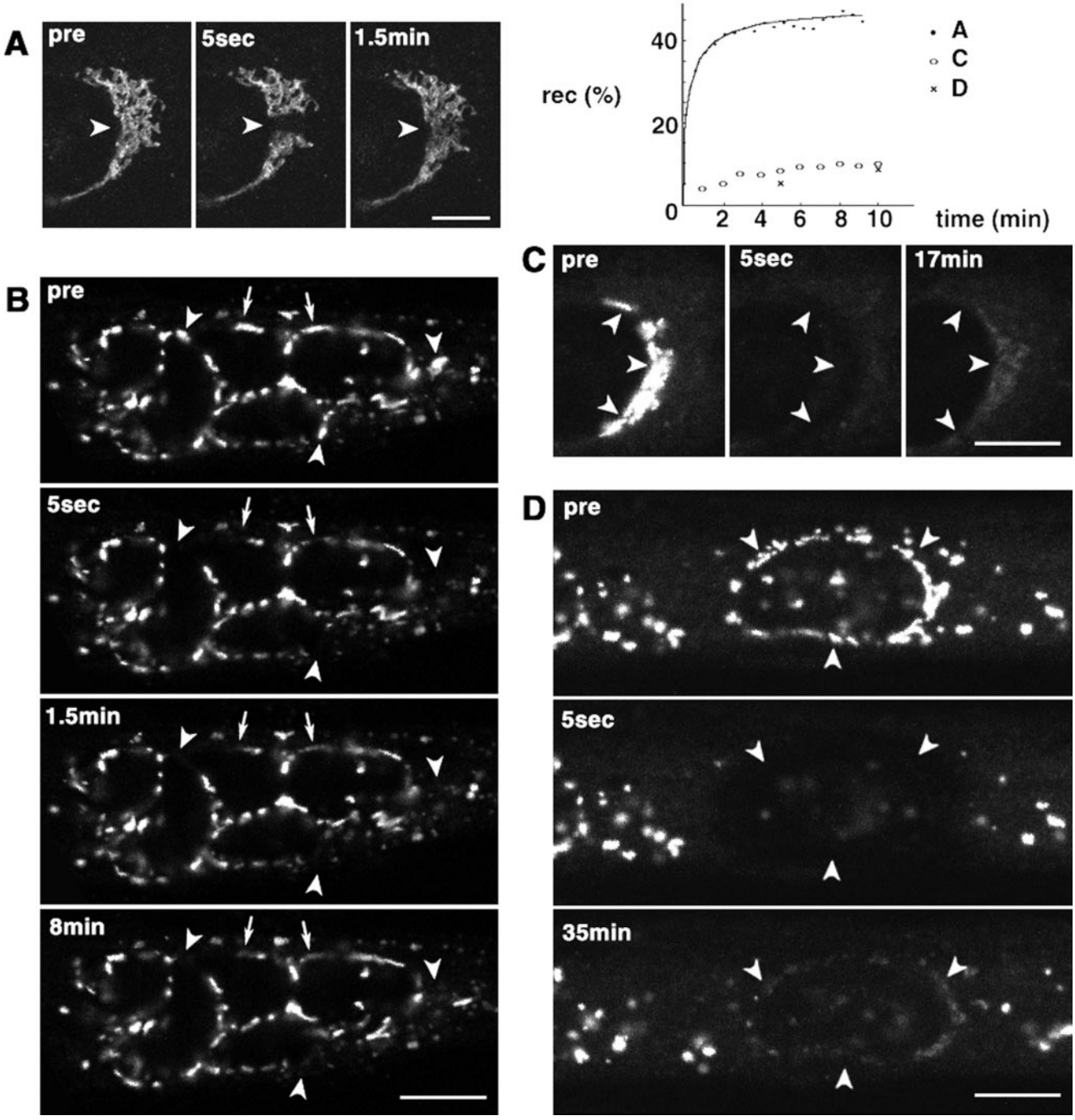

Figure 3. FRAP of mannosidase-GFP shows breakdown of continuity during differentiation. C2 cells that express man-GFP were pretreated with 25 μg/ml cycloheximide to inhibit protein synthesis and examined in the LSM 510 confocal microscope at 37°C. Each series of images shows a view before (pre), immediately after (5 s), and at different times after photobleaching. (A) Fast recovery of a 2-μm-wide band is observed in myoblasts (arrowhead). The fluorescence intensity of the bleached area was measured with NIH Image, and plotted and fitted in Kaleidagraph (see graph) to determine the diffusion coefficient (see MATERIALS AND METHODS and text). (B) In differentiated myotubes, fragments of individual elements (arrows) or whole elements (arrowheads) were photobleached. Recovery was fast for the fragments connected to a GFP source but absent for the whole elements. In C, the entire GC of a myoblast was photobleached and in D all elements of an extended area of myotubes. A slower and less complete recovery was observed, as plotted in the graph. Bars, 10 μm.

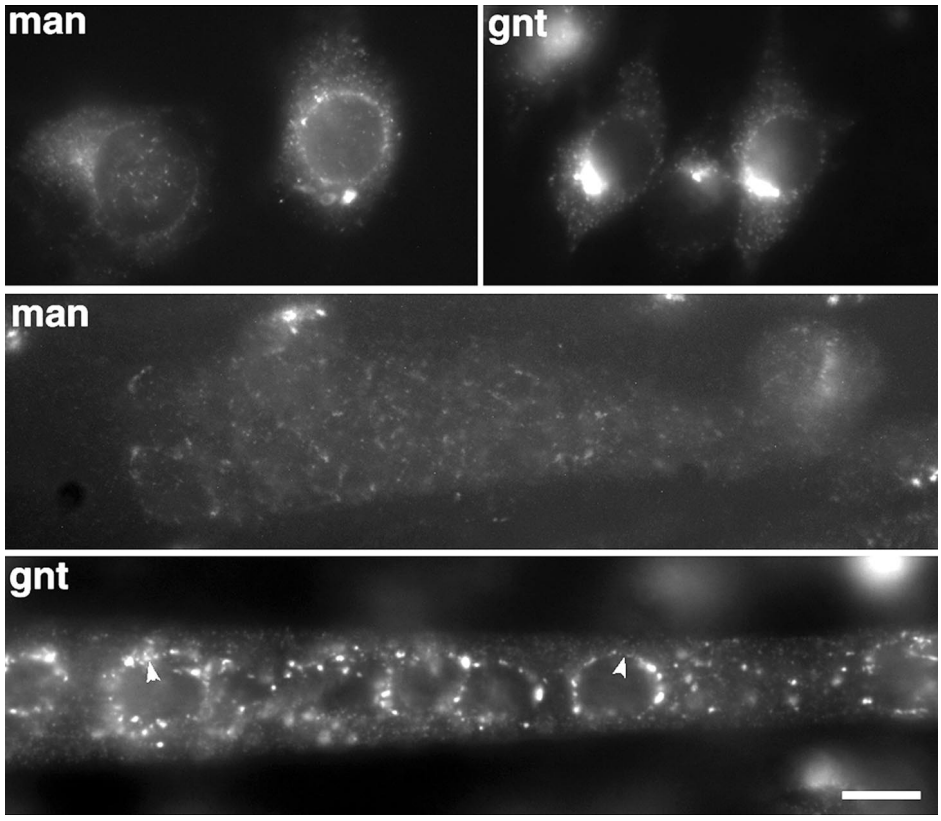

Figure 4. PLA2 inhibitor ONO redistributes GC proteins to the ER in both myoblasts and myotubes. The culture medium of C2 myoblasts (top row) or myotubes (bottom two rows) was replaced with serum-free medium supplemented with 15 μM ONO. After 2 h, cultures were stained with anti-mannosidase (man) or anti-giantin (gnt) and viewed by conventional fluorescence microscopy. The pattern shows a redistribution of mannosidase and giantin to the ER (compare with Figure 1 as control). In myotubes, ONO causes a decrease in the fluorescence intensity of both markers, especially noticeable with mannosidase; giantin staining appears more fuzzy and punctate than in control myotubes with a fine continuous staining detectable around some nuclei (arrowheads). Bar, 10 μm.

treatment, whether nocodazole was present or not (Figure 5, f and g). Because the pattern of giantin when it is near the ER exit sites in myotubes is indistinguishable from its normal pattern, we conclude that the distribution of ER exit sites, in myotubes, is similar to the distribution of the Golgi elements.

For direct observation of Golgi elements and ER exit sites, we double-stained C2 cultures with antibodies against the *cis*-GC protein GM130 (Nakamura *et al.*, 1996) and against the COPII protein Sec31p (Figure 6). In myoblasts, Sec31p forms small aggregates of uniform size distributed over the entire cytoplasm, in agreement with the distribution of the ER in these cells (Ralston and Hall, 1992) and with the pattern of COPII proteins in M1, Madin-Darby canine kidney, normal rat kidney (NRK), and other cells (Tang *et al.*, 1997; Shugrue *et al.*, 1999; Hammond and Glick, 2000; Stephens *et al.*, 2000). There is little colocalization of GC and ER exit sites, although the concentration of ER exit sites is higher in the perinuclear area. During differentiation, the pattern of Sec31p is reorganized (Figure 6). In myotubes it is found in larger aggregates of variable size, both along the nuclear membrane and in the cytoplasm. Many of these aggregates are next to Golgi elements. Each Golgi element is associated with a Sec31p aggregate but the reverse is not true: some small Sec31p aggregates similar to those of myoblasts are not associated with Golgi elements. In both myoblasts and myotubes, there is some background staining, possibly from a soluble pool of COPII proteins (Tang *et al.*, 1997). The same results were obtained with an antibody against the COPII protein Sec13p (our unpublished results).

In view of these changes, we wanted to verify that the structures stained by anti-Sec13p or anti-Sec31p in myotubes corresponded to morphologically defined ER exit sites. We labeled GM130 and Sec13p in myotubes with immunogold and examined the easily identifiable perinuclear area by EM in both labeled and unlabeled cells (Figure 7). In the unlabeled cells, evaginations of the outer nuclear membrane that extend toward the stacks of Golgi cisternae were frequently observed (Figure 7a). Staining with anti-GM130 (Figure 7b) confirmed the orientation of the *cis*-GC. In samples labeled with anti-Sec13p (Figure 7c), such evaginations were heavily labeled. No gold grain aggregates were observed close to the nuclear membrane of myoblasts (our unpublished results). Thus, EM evidence demonstrates that the changes in Sec13p pattern during differentiation does reflect a reorganization of the ER exit sites.

ER Exit Sites and Golgi Elements of Myotubes Are Localized near Microtubule Nucleation Sites

The Golgi complex of most interphase cells is kept at the centrosome by the action of minus end-directed microtubule motors (Corthesy-Theulaz and Pfeffer, 1992; Burkhardt *et al.*, 1997). The convergence of the microtubules nucleated at the single centrosome is therefore responsible for the compactness of the Golgi complex. During muscle differentiation, microtubule-nucleating proteins of the centrosome, such as pericentrin, redistribute from the unique centrosome to several "mini-centrosomes" and a perinuclear belt (Tassin *et al.*; 1985a,b; Ralston, 1993), all of which act as nucleation centers.

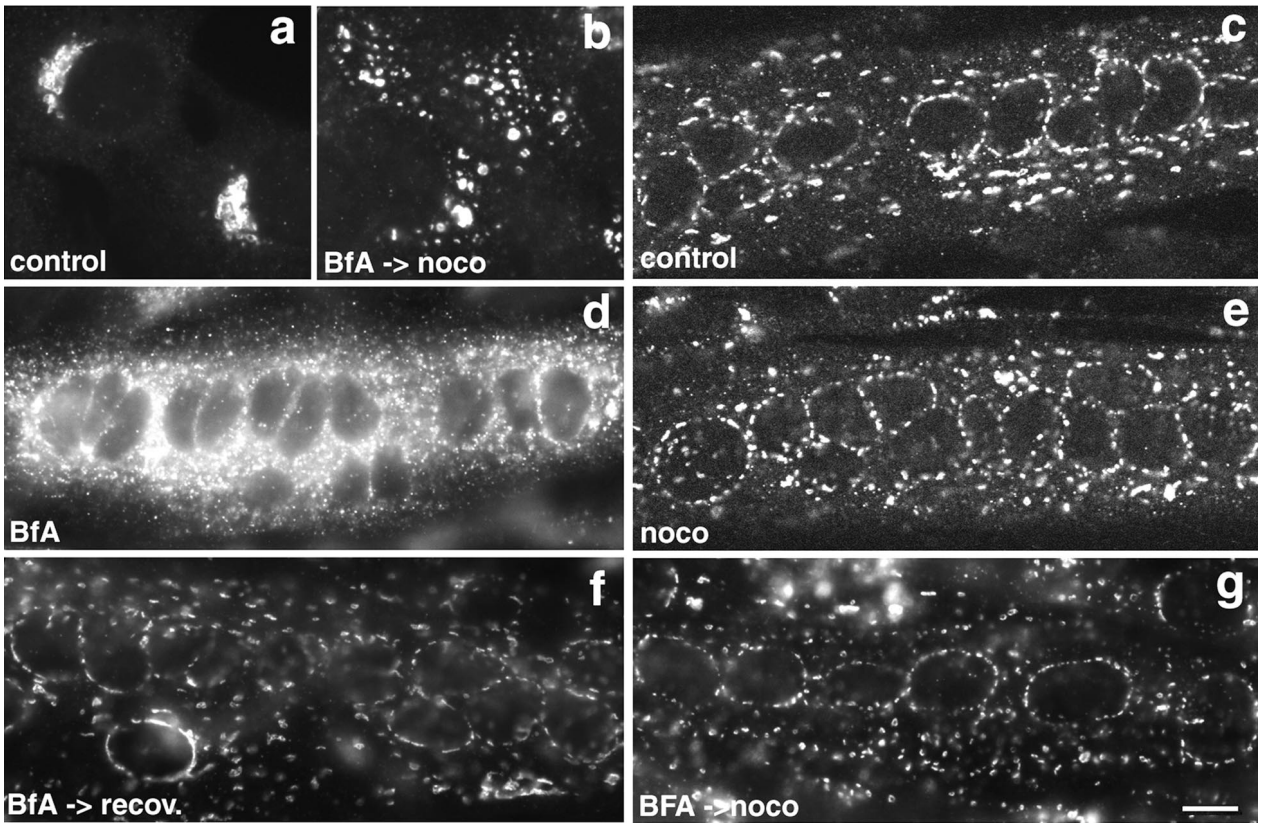

Figure 5. After treatment with BfA and recovery in nocodazole, the original GC pattern is recovered in myotubes but not in myoblasts. C2 myoblasts (a–b) or myotubes (c–g) were treated with 10 μg/ml BfA for 1 h (BfA), followed by 1-h recovery in the absence of drug (BfA → recov) or in the presence of 5 μg/ml nocodazole (BfA → noco). Also shown are control cells and a myotube treated with nocodazole alone (noco). At the end of the treatment, the cultures were stained with anti-giantin. BfA redistributes giantin to the ER, but the staining is more punctate than that of mannosidase, for which similar results were obtained. Treatment with nocodazole, as well as recovery from BfA in presence of nocodazole is known to redistribute GC proteins to the ER exit sites. In myoblasts recovered in the presence of nocodazole (b), the GC does not recover its initial distribution but remains fragmented compared with the control (a). In myotubes, giantin shows a similar distribution, whether it was redistributed to the ER exit sites (noco and BfA → noco), untreated (control), or recovered in drug-free medium (BfA → recov). Bar, 10 μm.

As a result, microtubules loose their convergence. At steady state, the network of microtubules in the myotube periphery is too dense to show anchoring points but a perinuclear ring can be observed (Figure 8A). To determine whether cytoplasmic GC elements are located close to nucleation centers, we then depolymerized the microtubules in nocodazole and allowed them to regrow for 5 min (Figure 8B). New microtubules formed a perinuclear ring and asters growing from the mini-centrosomes (Figure 8B). Double-staining for tubulin and Sec31p (Figure 8B) or giantin (our unpublished results) shows that aggregates of Sec31p or Golgi elements are localized near the microtubule nucleation sites. Quantitation of the confocal images showed that 85% of Sec31p dots (n = 827) and 84% of Golgi elements (n = 525) are found next to a focus of microtubule regrowth. The relative position of microtubule nucleation centers, Golgi complex, and ER exit sites is summarized in Figure 9 and used in the DISCUSSION as basis of two models to explain the Golgi complex changes during differentiation.

DISCUSSION

In this work, we examine the changes in the organization of the GC during muscle differentiation and propose that their mechanism is similar to that of the GC dispersal in nocodazole-treated cells.

The visualization of the GC changes in living cells has provided essential information on their timing and speed. It has also revealed, for the first time, cell motility-related dynamics of the GC. The arrest of the cells in nocodazole (our unpublished results) shows that their motility is microtubule-based, as reported for fibroblasts (Bershadsky and Vasiliev, 1993). The correlation between cell polarity and motility of C2 myoblasts is similar to that observed in fish keratocyte fragments (Verkhovsky *et al.*, 1999). The loss of polarity of the myoblasts as the Golgi complex becomes circular before fusion may facilitate the docking of the cells before fusion and the integration of the nucleus within a myotube. Changes in GC organization therefore must be

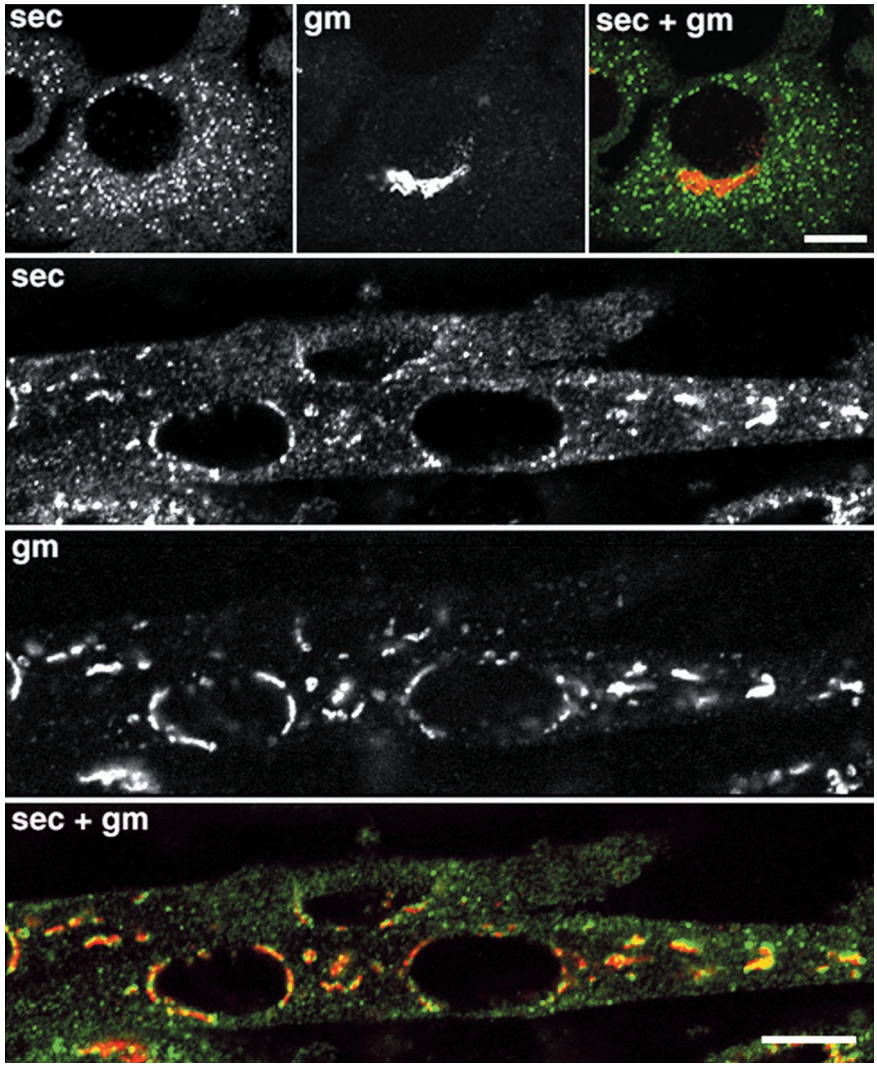

Figure 6. COPII complexes are reorganized during differentiation. C2 myoblasts (top row) or myotubes (bottom three rows) were double-stained with anti-Sec31p (sec) to label COPII complexes and anti-GM130 (gm) to label the GC, and observed in the confocal microscope. In myoblasts, Sec31p is distributed in puncta throughout the cell. In myotubes, it is found in aggregates of varying size prominently around nuclei. Superimposition of GM130 and Sec31p staining shows that each Golgi element is associated with one of these aggregates. The reverse is not true: some Sec31p aggregates are not associated with Golgi elements. There is also a background staining in both myoblasts and myotubes. Bars, 10 μm.

added to the number of important successive changes that take place before fusion during myogenesis (Andres and Walsh, 1996). In addition, we have shown that these changes, which, initially, seemed specific to the muscle lineage, in fact use pathways common to all mammalian cells.

To demonstrate that the GC becomes fragmented during differentiation, we turned to FRAP, which has been extensively used to examine organelle connectivity and dynamics (Cole *et al.*, 1996b; Ellenberg *et al.*, 1997; Terasaki, 2000). We measured a sharp loss of recovery following differentiation. We are confident that it is due to a loss of connectivity of the GC elements rather than to cell damage, because fast recovery of partially bleached elements could be observed within the same field (Figure 3B).

Next, we asked whether Golgi elements of myotubes are located at the ER exit sites, as are the Golgi complex fragments in nocodazole-treated cells. We found it to be so, but with a difference: in myotubes, both ER exit sites and Golgi complex elements are near the microtubule nucleation centers and thus near the minus ends of the microtubules. In other cells, Golgi complex fragments are found at the ER exit sites only in the absence of microtubules, because they lack the tracks to translocate toward the centrosome/microtubule nucleation center. The situation is summarized in cartoon form in Figure 9. Based on present knowledge, we can envisage two possible models to explain the changes that take place during differentiation.

The first model views the ER exit sites as static entities that occupy defined positions. The cycling Golgi complex proteins diffuse through the ER and leave at an ER exit site. The redistribution of Golgi components during differentiation can be explained in this model by assuming a relocation of the ER exit sites that brings them near the redistributed microtubule nucleation sites. Golgi complex proteins exiting the ER find themselves at the microtubule minus ends without need of translocation along the microtubules. They reform small stacks and stay at the ER exit sites. In favor of this model are reports that ER exit sites normally do not move much (Hammond and Glick, 2000; Stephens *et al.*, 2000). But cargo-independent redistribution of ER exit sites has never

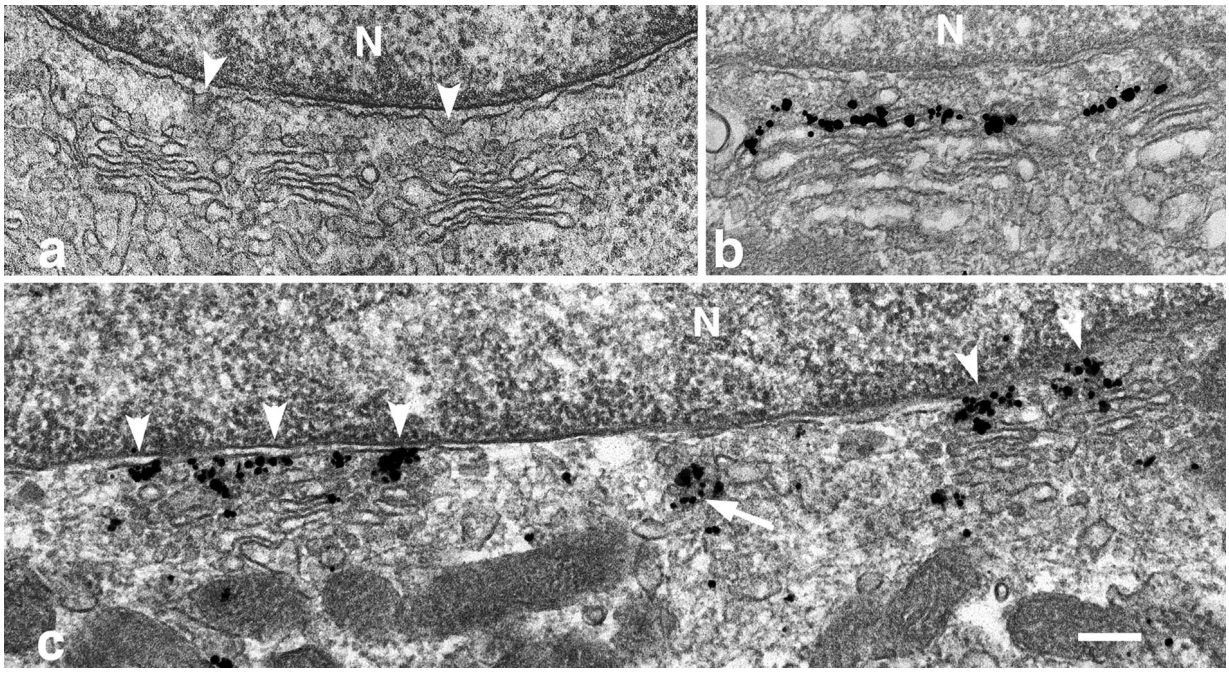

Figure 7. ER-GC area around the nuclei of myotubes is labeled with anti-Sec13p in immunogold EM. After 2 d in fusion medium, C2 cultures were fixed with 2% glutaraldehyde, processed, and embedded for EM (a); other cultures were fixed with a mixture of acrolein-p-formaldehyde (b and c), and immunolabeled with mouse anti-GM130 (b) or rabbit anti-Sec13p (c) followed by a gold-conjugated secondary antibody and silver enhancement (see MATERIALS AND METHODS). In the microscope, we focused on the perinuclear area, which is easily identifiable. Each panel shows small Golgi stacks next to a nucleus (N). Notice in a the evaginations of the outer nuclear membrane (arrowheads) pointing toward the GC, and the electron-dense coat associated with them, which resembles the COPII coat (Barlowe, 1998). (b) Position of the *cis*-GC labeled with anti-GM130. (c) Discrete aggregates of Sec13p covering the outer nuclear membrane and the adjacent area facing the *cis*-GC (arrowheads). Not every aggregate is asssociated with the nuclear membrane (arrow). Bar, 200 nm.

been reported. On the contrary, the formation of ER exit sites has been suggested to be modulated by cargo (Aridor *et al.*, 1999) and potential cargo receptors have been identified (Muniz *et al.*, 2000). In addition, Hammond and Glick (2000) have suggested that ER exit sites "proliferate" around the Golgi complex fragments in nocodazole, and Hobman *et al.* (1997) have shown that overexpression of a protein unable to leave the ER causes the accumulation of a membrane network enriched in COPII coat components. Most available evidence therefore suggests that ER exit sites are located in relation to their cargo rather than on their own. In addition, there is no obvious reason why ER exit sites would relocate to microtubule nucleation sites, whereas there is evidence that Golgi complex proteins do (Corthesy-Theulaz *et al.*, 1992).

The second model assumes that ER exit sites form de novo around the exiting cargo, here the GC proteins, which are then taken along microtubules toward the nucleation centers. Because there are now multiple nucleation centers and the microtubules do not converge any more, the Golgi complex proteins will form small, dispersed stacks of cisternae at the microtubule minus ends. What needs to be explained in this model is why the ER exit sites remain associated with the GC elements. In interphase cells, after cargo emerges from the ER, the COPII complex is rapidly replaced by the COPI complex (Aridor *et al.*, 1995; Scales *et al.*, 1997; Stephens *et al.*, 2000), which then takes the cargo further. However, it could be envisaged that, under specific circumstances, COPI does not replace COPII around the cargo and that COPII then remains associated with the cargo. In support of this model, we have observed relatively long-range, fast movements of a subpopulation of Sec13p-labeled ER exit sites in interphase myoblasts (~5 μm/s). We have also noticed a slower, concerted displacement of ER exit sites and mannosidase-GFP in nocodazole-treated myoblasts (Ralston and Lu, 2000). More experimental work will be needed to sort out these possibilities.

When ER exit site markers such as Sec13p are seen moving at high speed, it is likely that we are viewing COPII-coated vesicles detached from the ER. Slower movement, on the other hand, could reflect diffusion of the COPII coat in the ER membrane. Immunogold EM (Figure 7) was used to verify that Sec13p/Sec31p remain associated with the ER exit sites in myotubes as they are in other cells (Hammond and Glick, 2000; Stephens *et al.*, 2000). In addition, the immunofluorescent pattern of Sec13p and Sec31p in myotubes is similar to that of p58 in muscle fibers (Rahkila *et al.*, 1997). p58, the ER-Golgi intermediate compartment protein (Saraste and Svensson, 1991), is associated with COPII vesicles (Rowe *et al.*, 1996).

Finally, it is possible that the internal organization of the ER changes in preparation of the segregation of the sarcoplasmic reticulum from the ER. Rahkila *et al.* (1998) have shown that ER-to-GC trafficking of the G protein of vesicular stomatitis virus expressed in L6 muscle cells changes during differentiation with 50% of the protein retained in a pre-Golgi compartment in myotubes. The recycling Golgi com-

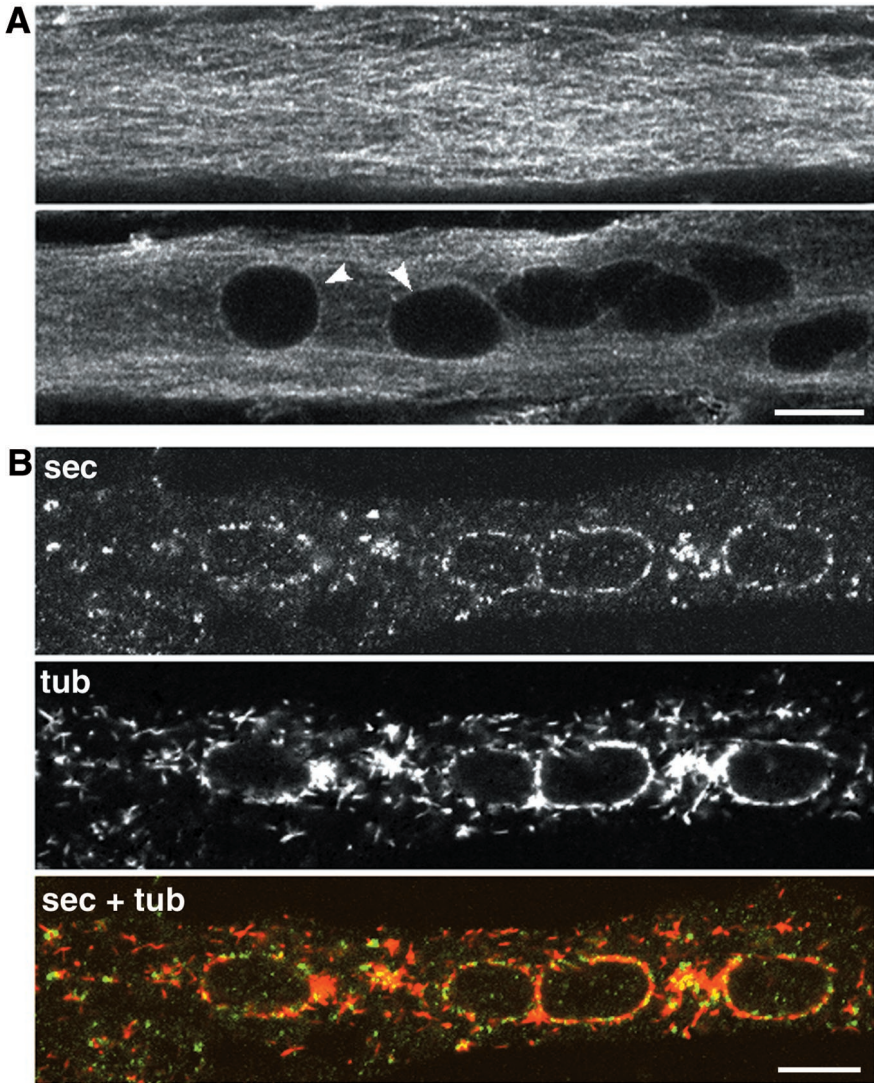

Figure 8. ER exit sites are close to microtubule minus ends in myotubes. Microtubules in untreated myotubes (A) and in myotubes in which microtubules had been left to recover for 5 min after depolymerization (B) were stained with anti-tubulin and observed in the confocal microscope. Close to the cell surface (A, top), there is a dense network of microtubules without clear nucleation points. In the core of the myotube (A, bottom), there is a perinuclear ring of tubulin (arrowheads) in addition to mostly longitudinal microtubules. (B) C2 myotubes were placed on ice for 10 min, and then warmed up at 37°C in nocodazole for 1 h to depolymerize the microtubules. Nocodazole was then washed out. After a 5-min recovery, cultures were fixed and stained with anti-tubulin (tub) and anti-Sec31p (sec). The microtubules had already reformed a perinuclear belt and had regrown from many cytoplasmic sites as well. Most ER exit sites (labeled with anti-Sec31p) are in proximity of a site of microtubule nucleation, which corresponds to the minus end of the microtubules. Bar, 10 μm.

plex proteins could then be rerouted and exit the ER in different places.

Cycling of Golgi complex proteins through the ER has been proposed by several groups to explain drug-induced or cell cycle-related changes in the Golgi complex. We now find that a strong argument can be made for a role of cycling of Golgi complex proteins in their reorganization during differentiation. Recovery of man-GFP fluorescence in the GC after total photobleaching and loss of man-GFP fluorescence in the GC after repeated photobleaching of the ER, in the absence of new protein synthesis, can only be explained by exchange between the two organelles. Both results are in agreement with those of Zaal *et al.* (1999). It has been suggested that the slow recovery in the absence of current protein synthesis could result from the delayed transport of GFP out of the ER. The absence of a large accumulation of unfolded mannosidase-GFP in the ER (Figure 1) rules out that explanation. In addition, no recovery can be detected for up to 5 h after complete photobleaching of a cell treated with cycloheximide (our unpublished results). Additional evidence in support of cycling also comes from experiments involving endogenous instead of transfected GC proteins, such as the redistribution to the ER of mannosidase and giantin during treatment with the PLA2 inhibitor ONO.

The time course of the GC changes during differentiation (1–2 h) is similar to that of the GC dispersal in nocodazole, and of the constitutive Golgi-to-ER recycling evidenced by ONO. It is then possible that all three follow the same pathway. However, Lee and Linstedt (2000) have data suggesting that the Golgi complex recycling in nocodazole is not the same as that of constitutive recycling. The GC changes observed here are slow in comparison with the dispersal of the GC in mitotic cells (Zaal *et al.*, 1999). We can rule out that the slow pace is due to poor health of the cultures or inadequate heating of the stage because we observed several instances of mitosis in our time-lapse recordings. In each case, the complete dispersal of the GC occurred from one frame to the next, i.e. within 15 min.

We have not been able, so far, to obtain evidence that blocking retrograde trafficking prevents the reorganization

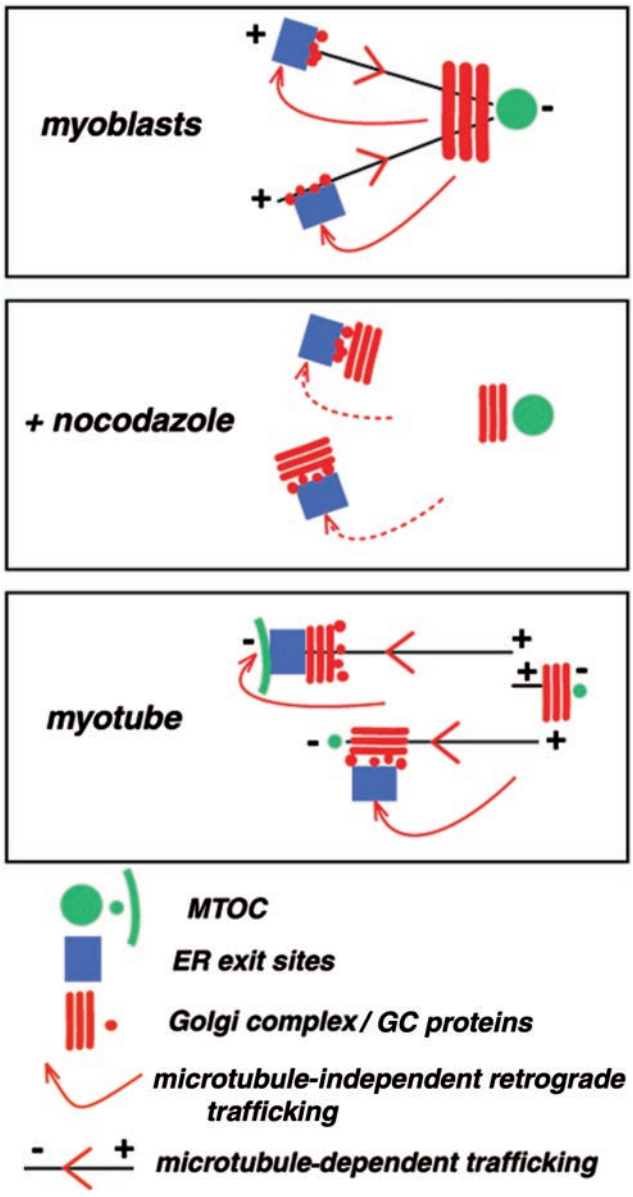

Figure 9. Relative organization of Golgi complex proteins, ER exit sites, and microtubules in myoblasts, nocodazole-treated myoblasts, and myotubes. In myoblasts, proteins of the GC constitutively cycle through the ER, which they leave at the ER exit sites to return to the GC in a microtubule-dependent translocation toward the minus ends. In nocodazole-treated myoblasts, the convergence of the GC is prevented by the lack of microtubules. Because retrograde trafficking is not interrupted, all GC proteins progressively end up at the ER exit sites where they form small stacks of cisternae. In myotubes, the microtubules are nucleated at multiple newly formed nucleation centers (MTOC) and do not converge. GC proteins and ER exit sites are both found at the microtubule minus ends. Two different models to explain the situation in myotubes are presented in the DISCUSSION.

of the GC. The favored experimental paradigm to demonstrate involvement of retrograde trafficking is the expression of a dominant-negative construct of the GTPase Sar1p (Aridor *et al.*, 1995), which is needed for COPII complex formation (Barlowe, 1998). This assay has been used by Shima *et al.* (1998), Storrie *et al.* (1998), and Zaal *et al.* (1999) to support opposite views (reviewed by Nelson, 2000). We expect that blocking exit from the ER during muscle differentiation would produce ambiguous results. Because GC proteins cycle through the ER in both myoblasts and myotubes, at about the same rate it takes for the differentiation process, they will be redistributed to the ER in all cells, regardless of their stage of differentiation, as was shown by the use of the PLA2 inhibitor ONO. Another PLA2 inhibitor, bromoenol lactone, blocks Golgi-ER cycling at the exit from the GC to the ER (Drecktrah and Brown, 1999) and therefore seemed promising. Unfortunately, it could not be used: after 4 h at the concentration needed in C2 cells, the drug affected microtubules, differentiation slowed down, and ER exit sites dispersed (our unpublished results). Dispersal of ER exit sites following a block of retrograde trafficking has also been observed with the protein kinase inhibitor H89 (Lee and Linstedt, 2000), suggesting that it may not be possible to observe ER exit site localization in the absence of retrograde trafficking. More specific reagents may become available as different routes for Golgi-to-ER transport are uncovered, such as a new Rab6-dependent retrograde pathway (White *et al.*, 1999).

The notion that the GC constantly recycles through the ER is not universally accepted (Shima *et al.*, 1998; Pelletier *et al.*, 2000; Seemann *et al.*, 2000). One of these articles argues that only the enzymes of the GC recycle, leaving out the GC matrix proteins, which include giantin. Our results do not support this model because we observe giantin redistribution to the ER by both BfA and ONO (Figures 4 and 5). The punctate pattern of giantin in the ER suggests that it remains in small clusters even in the ER, perhaps through links to other GC proteins. These and the rest of our results therefore support the notion of constitutive cycling of Golgi complex proteins through the ER and extend its involvement to a very different physiological situation, muscle differentiation.

It is possible to imagine the GC as a dynamic organelle, the state of which, in any cell type or situation, depends on a series of checkpoints along its cycle. This view is supported by the permanently fragmented organization of the GC in other cell types or organisms such as sea urchin embryos (Terasaki, 2000), plants (Dupree and Sherrier, 1998), and yeast (Wooding and Pelham, 1998; Rossanese *et al.*, 1999). The striking similarity between the GC organization of *Pichia pastoris* (Rossanese *et al.*, 1999) and of skeletal muscle, in particular, provides evidence for the wide applicability of this model.

ACKNOWLEDGMENTS

We are very grateful to the many colleagues who have generously provided us with antibodies or cDNAs. Confocal microscopy was done at the National Institute of Neurological Disorders and Stroke Light Imaging Facility and EM was done at the National Institute of Neurological Disorders and Stroke EM Facility. We are grateful to Wayne Rasband for help with the NIH Image software and to Christine A. Winters for technical help. We thank Drs. Nelson Cole, Carolyn Smith, and Jung-Hwa Tao-Cheng for critical reading of the manuscript and stimulating discussions. This work was supported by the National Institutes of Health Intramural program.

REFERENCES

Andres, V., and Walsh, K. (1996). Myogenin expression, cell cycle withdrawal, and phenotypic differentiation are temporally separable events that precede cell fusion upon myogenesis. J. Cell Biol. *132*, 657–666.

Aridor, M., Bannykh, S.I., Rowe, T., and Balch, W.E. (1995). Sequential coupling between COPII and COPI vesicle coats in endoplasmic reticulum to Golgi transport. J. Cell Biol. *131*, 875–893.

Aridor, M., Bannykh, S.I., Rowe, T., and Balch, W.E. (1999). Cargo can modulate COPII vesicle formation from the endoplasmic reticulum. J. Biol. Chem. *274*, 4389–4399.

Bannykh, S.I., Rowe, T., and Balch, W.E. (1996). The organization of endoplasmic reticulum export complexes. J. Cell Biol. *135*, 19–35.

Barlowe, C. (1998). COPII and selective export from the endoplasmic reticulum. Biochim. Biophys. Acta *1404*, 67–76.

Bershadsky, A.D., and Vasiliev, J.M. (1993). Mechanisms of regulation of pseudopodial activity by the microtubule system. Symp. Soc. Exp. Biol. *47*, 353–373.

Burkhardt, J.K., Echeverri, C.J., Nilsson, T., and Vallee, R.B. (1997). Overexpression of the dynamitin (p50) subunit of the dynactin complex disrupts dynein-dependent maintenance of membrane organelle distribution. J. Cell Biol. *139*, 469–484.

Cole, N.B., Ellenberg, J., Song, J., DiEuliis, D., and Lippincott-Schwartz, J. (1998). Retrograde transport of Golgi-localized proteins to the ER. J. Cell Biol. *140*, 1–15.

Cole, N.B., Sciaky, N., Marotta, A., Song, J., and Lippincott-Schwartz, J. (1996a). Golgi dispersal during microtubule disruption: regeneration of Golgi stacks at peripheral endoplasmic reticulum exit sites. Mol. Biol. Cell *7*, 631–650.

Cole, N.B., Smith, C.L., Sciaky, N., Terasaki, M., Edidin, M., and Lippincott-Schwartz, J. (1996b). Diffusional mobility of Golgi proteins in membranes of living cells. Science *273*, 797–801.

Corthesy-Theulaz, I., Pauloin, A., and Pfeffer, S.R. (1992). Cytoplasmic dynein participates in the centrosomal localization of the Golgi complex. J. Cell Biol. *118*, 1333–1345.

de Figueiredo, P., Drecktrah, D., Katzenellenbogen, J.A., Strang, M., and Brown, W.J. (1998). Evidence that phospholipase A2 activity is required for Golgi complex and trans Golgi network membrane tubulation. Proc. Natl. Acad. Sci. USA *95*, 8642–8647.

Doms, R.W., Russ, G., and Yewdell, J.W. (1989). Brefeldin A redistributes resident and itinerant Golgi proteins to the endoplasmic reticulum. J. Cell Biol. *109*, 61–72.

Drecktrah, D., and Brown, W.J. (1999). Phospholipase A(2) antagonists inhibit nocodazole-induced Golgi ministack formation: evidence of an ER intermediate and constitutive cycling. Mol. Biol. Cell *10*, 4021–4032.

Dupree, P., and Sherrier, D.J. (1998). The plant Golgi apparatus. Biochim. Biophys. Acta *1404*, 259–270.

Ellenberg, J., Siggia, E.D., Moreira, J.E., Smith, C.L., Presley, J.F., Worman, H.J., and Lippincott-Schwartz, J. (1997). Nuclear membrane dynamics and reassembly in living cells: targeting of an inner nuclear membrane protein in interphase and mitosis. J. Cell Biol. *138*, 1193–1206.

Gu, Y., Ralston, E., Murphy-Erdosh, C., Black, R.A., and Hall, Z.W. (1989). Acetylcholine receptor in a C2 muscle cell variant is retained in the endoplasmic reticulum. J. Cell Biol. *109*, 729–738.

Hammond, A.T., and Glick, B.S. (2000). Dynamics of transitional endoplasmic reticulum sites in vertebrate cells. Mol. Biol. Cell *11*, 3013–3030.

Hobman, T.C., Lemon, H.F., and Jewell, K. (1997). Characterization of an endoplasmic reticulum retention signal in the rubella virus E1 glycoprotein. J. Virol. *71*, 7670–7680.

Lee, T.H., and Linstedt, A.D. (2000). Potential role for protein kinases in regulation of bidirectional endoplasmic reticulum-to-Golgi transport revealed by protein kinase inhibitor H89. Mol. Biol. Cell *11*, 2577–2590.

Lippincott-Schwartz, J., Yuan, L.C., Bonifacino, J.S., and Klausner, R.D. (1989). Rapid redistribution of Golgi proteins into the ER in cells treated with Brefeldin A: evidence for membrane cycling from Golgi to ER. Cell *56*, 801–813.

Lucocq, J.M., and Warren, G. (1987). Fragmentation and partitioning of the Golgi apparatus during mitosis in HeLa cells. EMBO J. *6*, 3239–3246.

Muniz, M., Nuoffer, C., Hauri, H.P., and Riezman, H. (2000). The Emp24 complex recruits a specific cargo molecule into endoplasmic reticulum-derived vesicles. J. Cell Biol. *148*, 925–930.

Nakamura, N., Rabouille, C., Watson, R., Nilsson, T., Hui, N., Slusarewicz, P., Kreis, T.E., and Warren, G. (1996). Characterization of a cis-Golgi matrix protein, GM130. J. Cell Biol. *131*, 1715–1726.

Nelson, W.J. (2000). W(h)ither the Golgi during mitosis? J. Cell Biol. *149*, 243–248.

Pelletier, L., Jokitalo, E., and Warren, G. (2000). The effect of Golgi depletion on exocytic transport. Nat. Cell Biol. *2*, 840–846.

Rahkila, P., Luukela, K., Väänänen, K., and Metsikkö, K. (1998). Differential targeting of vesicular stomatitis virus G protein and influenza virus hemagglutinin appears during myogenesis of L6 muscle cells. J. Cell Biol. *140*, 1101–1111.

Rahkila, P., Väänänen, K., Saraste, J., and Metsikkö, K. (1997). Endoplasmic reticulum to Golgi trafficking in multinucleated skeletal muscle fibers. Exp. Cell Res. *234*, 452–464.

Ralston, E. (1993). Changes in architecture of the Golgi complex and other subcellular organelles during myogenesis. J. Cell Biol. *120*, 399–409.

Ralston, E., and Hall, Z.W. (1992). Restricted distribution of mRNA produced from a single nucleus in hybrid myotubes. J. Cell Biol. *119*, 1063–1068.

Ralston, E., and Lu, Z. (2000). Dynamics of ER exit sites and Golgi complex in doubly transfected live cells. Mol. Biol. Cell *11*, 281a.

Ralston, E., and Ploug, T. (1996). GLUT4 in cultured skeletal myotubes is segregated from the transferrin receptor and stored in vesicles associated with the TGN. J. Cell Sci. *109*, 2967–2978.

Robbins, E., and Gonatas, N.K. (1964). Histochemical and ultrastructural studies on HeLa cell cultures exposed to spindle inhibitors with special reference to the interphase cell. J. Histochem. Cytochem. *12*, 704–711.

Rogalski, A.A., and Singer, S.J. (1984). Associations of elements of the Golgi apparatus with microtubules. J. Cell Biol. *99*, 1092–1100.

Rossanese, O.W., Soderholm, J., Brooke, J.B., Sears, I.B., O'Connor, J., Williamson, E.K., and Glick, B.S. (1999). Golgi structure correlates with transitional endoplasmic reticulum organization in *Pichia pastoris* and *Saccharomyces cerevisiae*. J. Cell Biol. *145*, 69–81.

Rowe, T., Aridor, M., McCaffery, J.M., Plutner, H., Nuoffer, C., and Balch, W.E. (1996). COPII vesicles derived from mammalian endoplasmic reticulum microsomes recruit COPI. J. Cell Biol. *135*, 895–911.

Saraste, J., and Svensson, K. (1991). Distribution of the intermediate elements operating in ER to Golgi transport. J. Cell Sci. *100*, 415–430.

Scales, S.J., Pepperkok, R., and Kreis, T.E. (1997). Visualization of ER-to-Golgi transport in living cells reveals a sequential mode of action for COPII and COPI. Cell *90*, 1137–1148.

Seemann, J., Jokitalo, E., Pypaert, M., and Warren, G. (2000). Matrix proteins can generate the higher order architecture of the Golgi apparatus. Nature *407*, 1022–1026.

Shima, D.T., Cabrera-Poch, N., Pepperkok, R., and Warren, G. (1998). An ordered inheritance strategy for the Golgi apparatus: visualization of mitotic disassembly reveals a role for the mitotic spindle. J. Cell Biol. *141*, 955–966.

Shugrue, C.A., Kolen, E.R., Peters, H., Czernik, A., Kaiser, C., Matovcik, L., Hubbard, A.L., and Gorelick, F. (1999). Identification of the putative mammalian orthologue of Sec31P, a component of the COPII coat. J. Cell Sci. *112*, 4547–4556.

Stephens, D.J., Lin-Marq, N., Pagano, A., Pepperkok, R., and Paccaud, J.P. (2000). COPI-coated ER-to-Golgi transport complexes segregate from COPII in close proximity to ER exit sites. J. Cell Sci. *113*, 2177–2185.

Storrie, B., White, J., Rottger, S., Stelzer, E.H., Suganuma, T., and Nilsson, T. (1998). Recycling of Golgi-resident glycosyltransferases through the ER reveals a novel pathway and provides an explanation for nocodazole-induced Golgi scattering. J. Cell Biol. *143*, 1505–1521.

Tang, B.L., Peter, F., Krijnse-Locker, J., Low, S.H., Griffiths, G., and Hong, W. (1997). The mammalian homolog of yeast Sec13p is enriched in the intermediate compartment and is essential for protein transport from the endoplasmic reticulum to the Golgi apparatus. Mol. Cell. Biol. *17*, 256–266.

Tassin, A.M., Maro, B., and Bornens, M. (1985a). Fate of microtubule organizing centers during in vitro myogenesis. J. Cell Biol. *100*, 35–46.

Tassin, A.M., Paintrand, M., Berger, E.G., and Bornens, M. (1985b). The Golgi apparatus remains associated with microtubule organizing centers during myogenesis. J. Cell Biol. *101*, 630–638.

Terasaki, M. (2000). Dynamics of the endoplasmic reticulum and Golgi apparatus during early sea urchin development. Mol. Biol. Cell *11*, 897–914.

Turner, J.R., and Tartakoff, A.M. (1989). The response of the Golgi complex to microtubule alterations: the roles of metabolic energy and membrane traffic in Golgi complex organization. J. Cell Biol. *109*, 2081–2088.

Verkhovsky, A.B., Svitkina, T.M., and Borisy, G.G. (1999). Self-polarization and directional motility of cytoplasm. Curr. Biol. *9*, 11–20.

White, J., Johannes, L., Mallard, F., Girod, A., Grill, S., Reinsch, S., Keller, P., Tzschaschel, B., Echard, A., Goud, B., and Stelzer, E.H. (1999). Rab6 coordinates a novel Golgi to ER retrograde transport pathway in live cells [erratum in J. Cell Biol. (2000), 148]. J. Cell Biol. *147*, 743–760.

Wooding, S., and Pelham, H.R. (1998). The dynamics of Golgi protein traffic visualized in living yeast cells. Mol. Biol. Cell *9*, 2667–2680.

Yaffe, D., and Saxel, O. (1977). Serial passaging and differentiation of myogenic cells isolated from dystrophic mouse muscle. Nature *270*, 725–727.

Zaal, K.J., Smith, C.L., Polishchuk, R.S., Altan, N., Cole, N.B., Ellenberg, J., Hirschberg, K., Presley, J.F., Roberts, T.H., Siggia, E., Phair, R.D., and Lippincott-Schwartz, J. (1999). Golgi membranes are absorbed into and reemerge from the ER during mitosis. Cell *99*, 589–601.